University of Groningen

Cosmological reionization simulations for LOFAR

Thomas, Rajat Mani

IMPORTANT NOTE: You are advised to consult the publisher's version (publisher's PDF) if you wish to cite from it. Please check the document version below.

Document Version
Publisher's PDF, also known as Version of record

Publication date:
2009

Link to publication in University of Groningen/UMCG research database

Citation for published version (APA):
Thomas, R. M. (2009). *Cosmological reionization simulations for LOFAR*. s.n.

Copyright
Other than for strictly personal use, it is not permitted to download or to forward/distribute the text or part of it without the consent of the author(s) and/or copyright holder(s), unless the work is under an open content license (like Creative Commons).

The publication may also be distributed here under the terms of Article 25fa of the Dutch Copyright Act, indicated by the "Taverne" license. More information can be found on the University of Groningen website: https://www.rug.nl/library/open-access/self-archiving-pure/taverne-amendment.

Take-down policy
If you believe that this document breaches copyright please contact us providing details, and we will remove access to the work immediately and investigate your claim.

Downloaded from the University of Groningen/UMCG research database (Pure): http://www.rug.nl/research/portal. For technical reasons the number of authors shown on this cover page is limited to 10 maximum.

Download date: 06-05-2023

Chapter 7

Conclusion & Outlook

In order to succeed, your desire for success should be greater than your fear of failure.

Bill Cosby

7.1 Restating "the goal"

The primary purpose of the research that led to this thesis was the design and implementation of a fast algorithm for simulating the cosmological 21-cm signal from the Epoch of Reionization under a variety of astrophysical conditions. The work was expected to answer the following questions systematically:

- What are the ionization and heating patterns around sources with different continuum spectral energy distribution? How does radiative transfer including X-ray heating affect the IGM? What is the *sine qua non* of a given source type? For example, how are the signatures left by stars on their surrounding the IGM distinguished from those left by quasars? Can these signatures be observed in an experiment like LOFAR in isolation from or conjunction with instruments in other wavebands like ALMA? Can the algorithm developed here be used to design observational strategies for future EoR investigations as it has been for LOFAR? Can its use be extended to other contemporary and prospective experiments in the area? Answers to these questions involve trying to validate our predictions about (1) the typical frequency ranges (or redshift intervals) within which reionization accelerates and (2) the spatial scales that are most appropriate to the power on different scales of the signal and the various contaminants that affect it. These simulations are central to the task of establishing the robustness of various calibration schemes that will be employed in the experiment.

- Can the algorithm be made efficient enough to explore the entire parameter space introduced by astrophysical unknowns and produce maps large enough

to be a realistic recreation of the field that will be observed by LOFAR ($5^o \times 5^o$) ? These simulations are then to be used to provide a wide range of possible EoR signals as input to a "simulation pipeline" that will be used to study the telescope's response to the signal and validate the signal extraction schemes that are being developed.

In the sections that follow, we will describe our efforts towards answering the above questions.

7.2 Effect of miniquasars on IGM: Analytical approach

As a first exercise we analytically worked out a formalism to examine the feasibility of quasars heating of the IGM without violating the current observational constraints [Zaroubi et al., 2007]. Such heating is essential for the 21- cm emission from neutral hydrogen to be amenable to observation both before and during the EoR. We have shown that miniquasars with moderate black hole masses can heat the surrounding IGM up to the radii of a few comoving mega-parsecs.

Two scenarios were proposed for the evolution of black holes with different mass densities. For these two scenarios, we had three different quasar spectral templates: (i) a power-law with ionization UV radiation, (ii) a power-law without ionising UV radiation, and (iii) a Sazonov et al. [2004] type template. We have shown that quasars, with the exception of the models that have a 10% duty cycle, are not able to fully ionise the IGM – especially if one assumes the template that does not have ionising UV photons – while the SXRB constraint is satisfied. On the basis of the mass evolution history depicted here, we conclude that there is enough energy radiated by the quasars to heat the IGM by redshift 15. For example, for quasars with a power-law index of -1 and no ionising UV radiation and quasars with black hole masses of $10^{3-4} M_{\odot}$ can heat the IGM over a $\approx 0.1 - 1\mathrm{Mpc}$ comoving radius from the (mini-)quasar. (see Figure 2.5).

Curiously, in the case of the mass density evolution of black holes with a 10% duty cycle and rigid disk model, proposed by Begelman et al. [2006], this scenario does not violate the SXRB observational constraint. It produces about 10 ionising photons per baryon by $z = 6$, normally considered adequate to ionize the Universe. We also find that for a model in which the Universe ionizes suddenly at z=6, this scenario predicts a Thomson scattering optical depth of 0.075, consistent with the WMAP 3^{rd} year results.

The main result of this analytical exercise proved extremely encouraging for the new generation of low frequency radio telescopes such as LOFAR, MWA and PAST, which were designed to probe the high redshift IGM through its 21 cm emission,. It clearly shows that the quasar population could easily decouple the spin temperature from that of the CMB.

However, since the spin temperatures achieved are not very high, this means that the brightness temperature will carry the signatures not only of the ionized fraction and density fluctuations, but also those of variations in the spin temperature.

This complicates the interpretation of the observed brightness temperature in terms of its link to cosmological fields. Nevertheless, high spin-temperature bubbles are expected to overlap earlier than ionization bubbles, a factor that will mitigate this complication. Furthermore, one can turn this argument on its head and claim that these fluctuations will teach us more about the ionizing sources than about cosmology. An extended tail in the spin temperature will be a clear signature of power-law radiation, *i.e.*, of quasars, while a short tail will be a clear signature of thermal radiation, *i.e.*, of stars.

7.3 Modeling Radiative Transfer in 1-D

One of the purposes of the thesis is to simulate the signals from the EoR. The signals we are intent on capturing originate from neutral hydrogen atoms. Now, the purpose of the radiative transfer scheme, or for that matter any modeling scheme of the EoR, is to determine the distribution and evolution of the neutral hydrogen as a function of redshift. Thus, we needed a tool to calculate the extent of hydrogen ionization from a given distribution of radiating sources and neutral hydrogen density in the Universe. Towards achieving this goal, we built a radiative transfer scheme that followed the propagation of radiation through the IGM.

In Thomas and Zaroubi [2008] we reported the implementation of the radiative transfer code and some results of its application to the data of interest.

We developed a 1-D radiative transfer code for a detailed study of the influence of primordial black holes and Pop III stars on their surrounding environment. We have shown, and several other researchers agree with us, that black holes and/or Pop III stars have the potential to have been the primary source of ionization. Although the ionized regions around typical black holes are not shown to be convincingly different from those around Pop III stars modulo the resolution of telescopes like LOFAR, the heating profiles around these sources are significantly distinct. This difference is, in turn, reflected in the spin temperature of the system, which can be directly translated into the brightness temperature measured by the radio telescope.

Spin temperatures are coupled to kinetic temperature either through collision or through Lyα pumping. The strengths of these coupling terms are computed as a function of the radial distance from the source. Lyα photons couple spin temperature efficiently to kinetic temperature, making the brightness temperature insensitive to the CMB, at least for a substantial distance ($\approx 2 - 3Mpc$) away from the source. Recombination timescales are orders of magnitude lower than that of ionization. Therefore, an HII bubble remains ionized for a long period after the source of radiation has switched off. Besides, the temperature remains largely unchanged for a significant part of Hubble time because cooling processes typically involve two-body interaction that increases the timescales involved. Interestingly, in the case of miniquasars, a marginal increase is observed in the number of ionized bubbles even after the central ionizing source switches off. Collisional ionization is the dominant cause of this phenomenon. Collisional ionization occurs less in stars because stars lack high energy X-ray photons that heat the environment significantly and thus boost the process.

7.4 Properties of first objects and their impact

We used our 1-D radiative transfer code to explore the effect of having sources with different SEDs on their surrounding IGM. For miniqsos having a hard spectrum without the UV part, we observe an excess of HI fraction as a function of radius just before the main ionization front. This is interpreted as a result of the interplay between the increase of HeII and decrease of HeIII, which accelerates the HI recombination rate on the one hand and, on the other, decreases photon flux as a function of radius. This interpretation is supported by the observed weakening of the HI excess feature as a function of black hole mass. This phenomenon is not observed in miniqsos with a spectrum that has UV photons, which is due to the ionization efficiency of these photons.

The effect of the heating of the IGM around miniquasars as hypothesized by us was compared to the results of the analytical approach proposed by Zaroubi et al. [2007]. Figure 2.3 shows that the analytical approach, while in agreement within an order of magnitude, underestimates the kinetic temperature away from the centre by roughly a factor of up to 5. The difference between the results obtained by the two approaches is due to the fact that helium species cross-sections are not considered in the analytical approach. In fact, in order for the heating to be accurately calculated, one needs an exact knowledge of the abundance of both hydrogen and helium species averaged over their evolutionary history until the point of time one is specifically interested in. The analytical approach was simply not equipped to acquire such detailed knowledge.

The 1-D radiative code was also used to study thermal and kinetic Sunyaev-Ze'ldovich effects around quasars. Two cases are considered in which mass growth of the black hole is incorporated such that it leads to 10^8 and $10^9 M_\odot$ black holes at redshifts close to 6. The estimated values of temperature fluctuations are within the sensitivities of future missions like PLANCK.

We conclude that brightness temperature, which reflects the underlying ionization and heating around a source, is sensitive to many factors. The spectral energy distribution of the source, the range of energies spanned by the photons of these sources, their clustering properties, the photon escape fraction, the redshifts at which the sources turn-on, their lifetimes, and many other complex feedback mechanisms are some of the factors that influence the brightness temperature, which is the observable we are on the look out for. Thus, in order to span this large parameter space of possibilities, a 1-D radiative transfer code of the kind proposed here is not just useful, but quite essential.

7.5 The data cube for different scenarios

We have already emphasized the need to accommodate as yet unexplored scenarios within our simulation capabilities in order to ensure a robust and reliable pipeline that can deal with data acquired in the future. This necessitates speed and adaptability in the transfer codes realization of different scenarios. We built a scheme called

BEARS[1], in which a number of 1-D ionization profiles were catalogued for several luminosities, redshifts, densities and source spectra. These were subsequently coupled to an N-body simulation to obtain an approximation of a "standard" 3-D radiative transfer code. The results obtained were validated using CRASH, a full 3-D radiative transfer code with ray tracing. The agreement between the two methods was excellent for early redshifts ($z > 8$), but, as expected, discrepancy crept in towards lower redshifts. Several visual comparisons of the slices of different boxes and three different statistical tests of similarity between the simulations were conducted. We are happy to report that our results are congruent with those obtained from standard codes along expected lines.

Many snapshots (≈ 75) were used between redshifts 15 and 6. These were subjected to radiative transfer as described in the preceding sections. These snapshots were then used to make a contiguous cube running from redshift 6 to redshift 12. In terms of observation frequency, the cube spans 115 MHz to 200 MHz with a frequency resolution matching that of LOFAR, about one MHz. Cubes were generated for scenarios involving only stars or quasars, and diagnostics are provided to quantitatively differentiate between them. For both models the variance in δT_b peaked at around 160 MHz. Although neither may reflect reality exactly, these scenarios demonstrate the use of the techniques we have developed to span large parameter spaces of variables.

The PDF of δT_b (see Fig. 5.13) provides a statistical discriminant between the different source scenarios and could be used in future applications to obtain the statistical detection of the signal.

The cubes generated provide δT_b as a function of frequency. The cubes were then averaged over a bandwidth of 1 MHz and convolved with the beam pattern of LOFAR to understand the distortions caused by incomplete sampling with an interferometer. Even if the images were blurred by the operation, the overall characteristics of the signal remained detectable. Although the behaviour of the variance of the signal before and after the convolution remained the same (except that the latter had average lower values), the image/slice entropy showed a very different behavior. In the former case, i.e., before convolution, the image entropy remained almost flat throughout the frequency range whereas post-convolution, the entropy steeply rose at around 160 MHz.

It is important to mention here that, although in principle the ionized bubbles do move with a peculiar velocity $v_r(z) = v_r(0)(1+z)^{-1/2}$, where $v_r(0)$ is the typical peculiar velocity of galaxies at redshift zero, assuming $v_r(0) \approx 600$km/s, a redshift 10 object would have a peculiar velocity of 200 km/s. For a typical lifetime of the source considered, i.e., 10 Myr, this corresponds to motion of about a couple of kpc. This is an order of magnitude less than the resolution of the simulation box at that redshift. Therefore we ignore this effect. On the other hand, we have taken into account the effect of redshift distortions whose effects are relatively more important.

The simulations and comparisons reported in this thesis have focused on purely stellar or quasar sources, but it is plausible that the early sources of reionization were a mixture of stars and quasars or other as yet unknown sources. It is therefore impor-

[1] **B**ubble **E**xpansion **A**round **R**adiative **S**ources

tant to simulate reionization caused by a combination of these sources, taking into account their clustering properties. The simulations presented in this thesis did not take into account the constraints on the population of ionizing sources imposed by various measurements like the infrared excess in the case of stars and the soft X-ray excess for quasars. Apart from the ionization patterns induced by these sources, the δT_b maps will also depend on the kinetic temperature which is coupled to the spin temperature via collisions or Ly-α pumping. Hence, it is imperative that we include these temperature effects on the IGM. We will shortly communicate the results of the combination of sources and the effect of the temperature in an article in preparation at present. (Thomas et al., *in prep*).

One of the main astrophysical hurdles for the detection of EoR signals is the existence of prominent Galactic and extragalactic foregrounds. The difference between the mean amplitudes of the EoR signal and the foregrounds is generally expected to be 4 to 5 orders of magnitude, but an interferometer like LOFAR measures the fluctuations different by 'only' three orders of magnitude [Jelić et al., 2008].

7.6 Including X-ray heating in BEARS

Thus far brightness temperatures from the EoR was calculated based on the assumption that the $T_{spin} >> T_{CMB}$. This might be a valid assumption towards the end of reionization, but certainly less realistic at the beginning. In order to self-consistently calculate δT_b as a function of redshift, we have first to include the calculations of the kinetic temperature and the Jα flux within the simulation. Inclusion of heating within our algorithm allowed for the modelling of more realistic scenarios in which the reionization was achieved by hybrid model of stars and power-law sources, instead of only either one of them. Thus the focus of this chapter was two fold. One, to introduce the algorithm to incorporate heating (including X-ray heating) in BEARS and discuss its application to two cases of reionization and heating, i.e., for blackbody (stellar) and power-law (quasar) type sources. Secondly, this algorithm was used to study the influence of a hybrid population of stars and quasars as reionizing sources.

Heating of the IGM by the reionizing sources was folded into BEARS following a procedure of embedding spheres of "temperature" bubbles, much like the algorithm used to obtain the ionized fraction. Overlaps were treated by considerations of the conservation of energy. The BEARS algorithm implemented here is extremely quick. This implies, that various scenarios of reionization can be implemented and tested for observational signatures in the redshifted 21-cm emission.

It was clear from the simulations that quasar type sources are not only very efficient in increasing the kinetic temperature of the IGM, the Lyα flux produced by them is sufficient enough to drive T_{spin} away from the CMB temperature, rendering the environment around the source visible in δT_b. Therefore, if a quasar with a blackhole in the range $> 10^6\ M_\odot$ is within the observing window of LOFAR, the brightness temperature produced by it would be high enough to be visible in the experiment. This is not the case for stars because the sizes of the region and the extent of heating both are much smaller than that of the quasar.

Stars and quasars were combined in a hybrid model of reionization. Every dark matter halo was embedded with both a quasar and a stellar component. The relation between the two was set reflecting the Magorrian relation we observe today. The quasar masses were limited such as not to violate the black hole mass densities estimates by Volonteri et al. [2008b].

Results from all these simulations, i.e., stars, quasars and the hybrid we used to create reionization histories and the observational cube in each of the cases. Stark differences can be found in each of these simulations. Statistical studies of the differences in various models are deferred to another paper.

7.7 Future work

There are two ways of looking at what needs to be done next:

1. refinements in the current simulations and
2. using the existing simulations for various studies/predictions

7.7.1 Refining the simulations

One of the urgent requirements is to extend the code to be able to simulate extremely large boxes. The need for efficient simulations for the EoR was explicitly expressed in Thomas and Zaroubi [2008], Thomas et al. [2008] andMesinger and Furlanetto [2007]. Most simulations of the EoR are performed on boxes that are up to 100 comoving Mpc on each side [Mellema et al., 2006, Ciardi and Madau, 2003].

At a redshift of 10, the field-of-view (FoV) of LOFAR or MWA, which is $\approx 5^o \times 5^o$, corresponds to a comoving length of $\approx$ 800 comoving Mpc. The radial comoving distance from redshift 6 to 12 is in the order of 1600 Mpc. To provide simulated data sets for the ranges (spatial & frequency) observed by LOFAR or MWA, we need to stack $\sim$ 8 boxes end-to-end along right ascension (RA) and declination (Dec) and $\sim$ 16 boxes along the frequency direction. This approach artificially introduces correlations on scales larger than the size of the simulation. In order to develop a reliable scheme of data analysis and in order to perform proper statistics (for example, when correlating the EoR data sets with other data sets like that of the CMB maps by PLANCK), it is essential to simulate data sets that are devoid of such artifacts.

7.7.2 Synergy across the electromagnetic spectrum

The next decade will witness some of the largest projects envisioned in radio astronomy with arrays like the LOFAR, MWA, PAPER, CORE, and ALMA followed by the SKA [2] . Except in the case of ALMA, all these experiments aim at detecting and

[2]Acronyms: **LOFAR** LOw Frequency ARray, **MWA** Murchison Widefield Array, **PAPER** Precision Array Probing the Epoch of Reionization, **CORE** Cosmic Reionization Experiment, **ALMA** Atacama Large Millimeter Array, **SKA** Square Kilometer Array, **VISTA** Visible & Infrared Survey Telescope, **LSST** Large Synoptic Survey Telescope, **JWST** James Webb Space Telescope, **HST(NICMOS)** Hubble Space Telescope (Near Infrared Camera and Multi-Object Spectrometer).

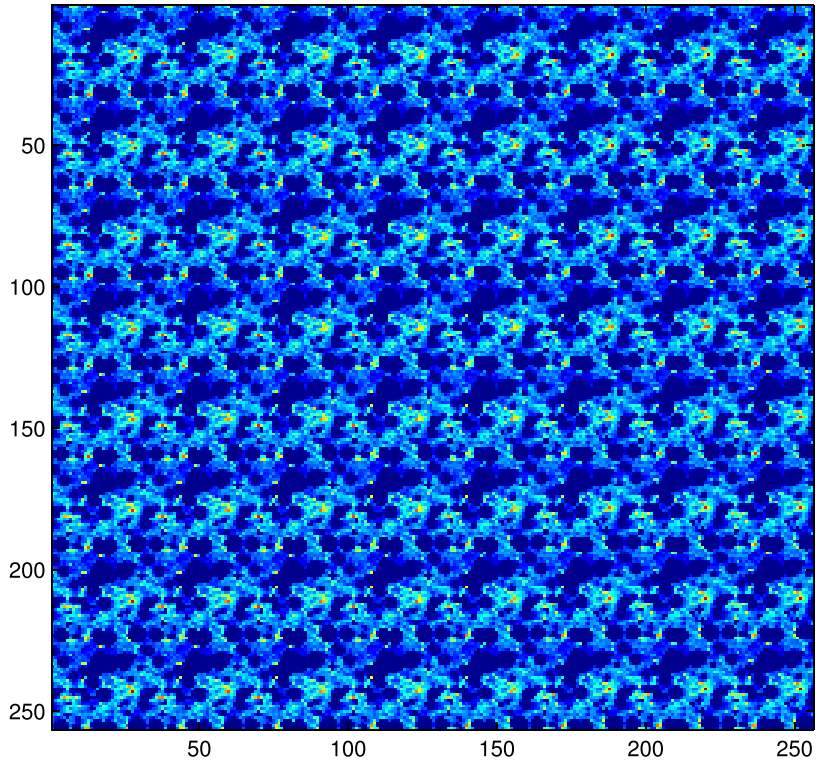

Figure 7.1: *Figure above demonstrates the problem with stacking numerous images of the same simulation to create the mosaic of a large field. The high degree of periodicity above the scale of one box-size is potentially damaging to the task of calculating reliable estimates of cross-correlations of this simulation with other datasets.*

imaging redshifted 21-cm emission from the EoR.

While these 21-cm radio observations will provide us with a tomographic map of the distribution of neutral hydrogen in the Universe, showing ionized regions as "Strömgren bubbles" in the data set, complementary deep near/mid-IR imaging from ground-based survey instruments like the VISTA, the LSST, the Subaru Telescope and space-based instruments like deep HST(NICMOS)/JWST [2] will provide detailed information on the radiative sources (eg., galaxies, QSOs, Lyα emitters etc.) that reside in these bubbles.

The reason why we make observations in the near (mid)-IR is that the Lyα (Hα) emitters restframe 1216 (6563) A^o redshift beyond 1.2 micron (6.5 micron) at z>9,

where reionization takes place the most Komatsu et al. [2008]. Because these sources ionize the neutral hydrogen around them, there should be a clear anti-correlation between the redshifted 21-cm and near/mid-IR observations Wyithe et al. [2007].

Many new questions about the infancy of the Universe (the 1st billion years) can be answered more precisely using these two data sets than was possible till now. To briefly mention a few; What is the reionization history of the Universe? What are the cosmological parameters: H(z), Ω_b, Ω_m,n ? What is the nature of the first radiation sources? How strong was the primordial magnetic field? What are the physical properties of dark matter particles? Has there been any variation in the fine structure constant? [Madau et al., 1997, Ciardi and Madau, 2003, Loeb and Zaldarriaga, 2004, McQuinn et al., 2005, Barkana and Loeb, 2005, Pritchard and Furlanetto, 2006, Tashiro and Sugiyama, 2006, Shchekinov and Vasiliev, 2006, Khatri and Wandelt, 2007, Kanekar et al., 2005]

It may be justifiably asserted that the data sets generated as part of our effort to simulate the entire FoV of an EoR experiment can be used for other larger future purposes. For example, they might provide useful estimates of the observability of the Sunyaev-Zeldovich effect caused by early black holes for ALMA, and cross-correlate the data sets with simulations of the CMB maps that will be obtained by PLANCK to (i) study the nature of the reionization sources; (ii) reconstruct the cosmic reionization history; and (iii) infer the mean cosmic ionization level at any redshift [Salvaterra et al., 2005]. Also Spaans and Meijerink [2008] recently pointed out how ALMA can be used to detect CO transitions at high $\mathcal{J} > \infty\bigtriangledown$ which acts as a tracer to x-ray radiation. This can then be used in conjunction with the 21-cm survey to study the environment around the x-ray source.

7.7.3 Remarks

Thus, our immediate goal involves

- To simulate the entire field of view of LOFAR, which is $5^o \times 5^o$ or box-size with 1 Gpc comoving length on one side,
- To include Lyα radiative transfer, and
- To cross-correlate our data with other data sets (CMB, ALMA, mid/near-IR).

As for the LOFAR experiment itself, the future is here. The infrastructure is being setup and algorithms are being developed, tested, and commissioned. The experiments begin September 2009.